Nonlinear Dynamic Analysis of Cantilever Tube Conveying Fluid with System Identification

Jae-Hoon Lim
School of Mechanical Engineering, Sungkyunkwan University, 300, Chunchun-dong, Jangan-gu, Suwon, Kyunggi-do, 440-746, Korea
Goo-Choong Jung
Daelim Industrial Co., Ltd. 17-5, Yoido-dong, Youngdungpo-gu, Seoul 150-010, Korea
Yeon-Sun Choi*
School of Mechanical Engineering, Sungkyunkwan University, 300, Chunchun-dong, Jangan-gu, Suwon, Kyunggi-do, 440-746, Korea

The vibration of a flexible cantilever tube with nonlinear constraints when it is subjected to flow internally with fluids is examined by experimental and theoretical analysis. These kinds of studies have been performed to find the existence of chaotic motion. In this paper, the important parameters of the system leading to such a chaotic motion such as Young's modulus and the coefficient of viscoelastic damping are discussed. The parameters are investigated by means of system identification so that comparisons are made between numerical analysis using the design parameters and the experimental results. The chaotic region led by several period-doubling bifurcations beyond the Hopf bifurcation is also re-established with phase portraits, bifurcation diagram and Lyapunov exponent so that one can define optimal parameters for system design.

Key Words : Bifurcation Diagram, Period Doubling Bifurcation, Phase Plane Plot, Cantilever Tube, Constraint Bar, Chaotic Motion, System Identification, Lyapunov Exponent

1. Introduction

It is widely known from various experiments and analyses that a flexible tube conveying fluid is destabilized by buckling or flutter when the fluid flows beyond a critical velocity. It plays an important role to analyze the dynamics of the tube as designing of the piping system subjected to disturbance by fluids.

So far, various studies have been made on the stability of the tube system. These studies began with a research by Ashley and Haviland (1950) to investigate the vibration in the Trans-Arabian Pipeline. Benjamin (1961) verified that the dynamic characteristic of the articulated pipes has not any effect on friction between pipe and internal fluid. Paidoussis (1970) examined the stability of a standing cantilever tube and a hanging cantilever tube, respectively. He showed that for sufficient high flow velocity the hanging tube flutters, on the contrary the standing tube loses its stability by buckling due to the weight of the tube itself as well as flutter. Sugiyama (1985) found the critical flow velocity along the stiffness and position of a supported spring in the horizontal cantilever tube.

In addition to the above researches, several studies have been made on investigating such a chaotic region concerning the nonlinearity of the system. Paidoussis and Moon (1988) established that a chaotic oscillation occurs in the tube re-

* Corresponding Author,
E-mail : yschoi@yurim.skku.ac.kr
TEL : +82-31-290-7440; **FAX** : +82-31-290-5849
School of Mechanical Engineering, Sungkyunkwan University, 300, Chunchun-dong, Jangan-gu, Suwon, Kyunggi-do, 440-746, Korea. (Manuscript **Received** June 30, 2003; **Revised** September 16, 2003)

strained within a gap between the tube and a motion constraint by experiments and numerical analyses. Thereafter, Paidoussis (1989) investigated which parameters affect a tube system to bifurcation and chaotic motion with the calculation of the largest Lyapunov exponents. Choi (1988) investigated the motion within a constraint, which makes a piecewise-linear system. Jin (1997) investigated the effect of the spring constant, which restrains the motion of the tube, and some other parameters on the dynamics of the system.

As the concern with chaotic motion in nonlinear system has been growing in recent years, a number of studies have been focused on the possibility of the existence of chaotic motion on the tube system conveying fluid. However there has not been any studies that tried to set up the parameters of the system such as the modulus of elasticity and the coefficient of viscoelasticity, having an important effect on the dynamic behavior of the tube. Since these parameters are sensitive to the environments of the system, the temperature and the humidity, and a term of application, etc., these can be varied and give rise to induce the nonlinear characteristic of the tube, i.e., bifurcation and chaotic motion.

For this reason, in this paper, the parameters are estimated with system identification through the data obtained by experiments and it is performed to examine the difference between the result of the estimation and a numerical analysis so that one can define the value of the parameters close to a practical condition.

2. Equation of Motion of a Cantilever Tube

A tube utilized in this study is a cantilever tube having its length, L as shown in Fig. 1. The mass per unit length of the tube is, the flexural rigidity of the tube, EI, the fluid mass per unit length is M and the fluid flows along the internal tube with the velocity, U and is discharged at its free end. The tube hanging vertically is undeformed initially along the x-axis.

The fluid being conveyed is assumed to be

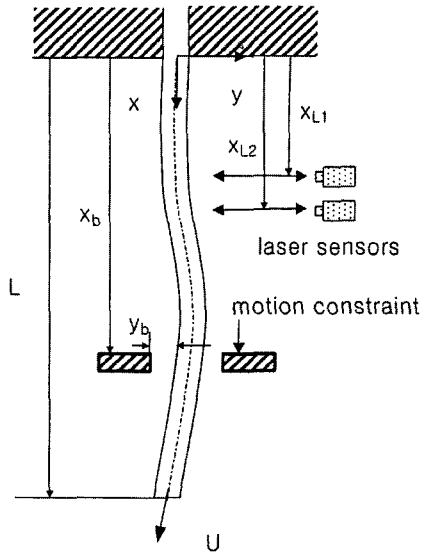

Fig. 1 Schematic of the system

incompressible, of a steady-flow, and having a uniform velocity profile. In addition, since the diameter of the tube is smaller than the length of it and the motion of the tube is planar, an Euler-Bernoulli beam approximation is applied, which neglects the rotary inertia and shear deflection in the tube.

The equation of motion of the cantilever tube can be derived by a force balance method as following (Paidoussis et al., 1991).

$$EI\frac{\partial^4 y}{\partial x^4}+E^*I\frac{\partial^5 y}{\partial x^4\partial t}+[MU^2-(M+m)(L-x)g]\frac{\partial^2 y}{\partial x^2}+2MU\frac{\partial^2 y}{\partial x\partial t}+(M+m)g\frac{\partial y}{\partial x}+(M+m)\frac{\partial^2 y}{\partial t^2}+\kappa(y-0.5(|y+y_b|-|y-y_b|))\delta(x-x_b)=0 \quad (1)$$

where t denotes the time, g the gravitational acceleration, E^* the coefficient of Kelvin-Voigt damping, and the lateral displacement of the tube is $y(x, t)$. And is the stiffness of the constraint, x_b the position of the constraint, y_b the gap between the tube and the constraint, δ is the Dirac delta function.

The dimensionless equation with Eq. (3) yields,

$$[1+a(\partial/\partial\tau)]\eta''''+[u^2-\gamma(1-\xi)]\eta''+2\beta^{1/2}u\dot{\eta}'+\gamma\eta'+\ddot{\eta}+\kappa\left(\eta-\frac{1}{2}(|\eta+\eta_b|-|\eta-\eta_b|)\right)\delta(\xi-\xi_b)=0 \quad (2)$$

$$\eta=\frac{y}{L},\ \xi=\frac{x}{L},\ \tau=\left(\frac{EI}{M+m}\right)^{1/2}\frac{t}{L^2},$$
$$u=\left(\frac{M}{EI}\right)^{1/2}UL,\ \beta=\frac{M}{M+m},\ \gamma=\frac{M+m}{EI}gL^3, \quad (3)$$
$$\kappa=\frac{\kappa L^3}{EI},\ \alpha=\left(\frac{EI}{M+m}\right)^{1/2}\frac{a}{L^2},\ \alpha=\frac{E^*}{E},$$
$$(\ )'=\partial(\ )\partial\xi,\ (\dot{})=\partial(\ )/\partial\tau$$

Then, the Gallerkin's method is utilized on Eq. (2) to yield the ordinary differential equation,

$$\eta(\xi,\ \tau)=\sum_i\phi_i(\xi)\,q_i(\tau) \quad (4)$$

where the comparison functions, $\phi_i(\xi)$, are the cantilever beam eigenfunctions. Substituting Eq. (4) into Eq. (2) and integrating through the length of the tube, one obtains,

$$\{\ddot{q}\}+[C]\{\dot{q}\}+[K]\{q\}+\{F(q)\}=\{0\} \quad (5)$$

The elements of matrices, $[C]$, $[K]$, and $[F(q)]$, are, respectively,

$$C_{sr}=\alpha\lambda_r^4\delta_{sr}+2\beta^{1/2}ub_{sr},\ K_{sr}=\lambda_r^4\delta_{sr}+u^2c_{sr}+\gamma e_{sr},$$
$$F_r=\kappa\Big[\sum_r\phi_r(\xi_b)\,q_r-\frac{1}{2}\Big(\Big|\sum_r\phi_r(\xi_b)\,q_r+\eta_b\Big| \quad (6)$$
$$-\Big|\sum_r\phi_r(\xi_b)\,q_r-\eta_b\Big|\Big)\Big]\phi_r(\xi_b)$$

$$b_{sr}=\begin{cases}4/[(\lambda_s/\lambda_r)^2+(-1)^{r+s}], & r\neq s\\ 2, & r=s\end{cases},$$
$$c_{sr}=\begin{cases}4(\lambda_r\sigma_r-\lambda_s\sigma_s)/[(-1)^{r+s}-(\lambda_s/\lambda_r)^2], & r\neq s\\ \lambda_r\sigma_r(2-\lambda_r\sigma_r), & r=s\end{cases}, \quad (7)$$
$$e_{sr}=\begin{cases}\{4(\lambda_r\sigma_r-\lambda_s\sigma_s+2)(-1)^{r+s}\\ \quad -2[1+(\lambda_s/\lambda_r)^4]b_{sr}\}/\{1+(\lambda_s/\lambda_r)^4\}\\ \quad -c_{sr}, & r\neq s\\ \{2-1/2c_{sr}, & r=s\}\end{cases}$$

where, δ_{sr} in Eq. (6) is Kronecker's delta.

The eigenvalues of the system are plotted in Fig. 2 on the assumption that the system has one-degree-of-freedom (a) and two-degree-of-freedom (b). The arrows denote the increasing flow velocity. Figure 2 shows that the system is stable for all the flow velocity in (a), but the econd complex conjugate pair of four eigenvalues of the system govern the unstable behavior of the system in (b). In detail, the system becomes unstable by oscillatory behavior, i.e., flutter when the real values of second pair of eigenvalues, $\mathrm{Re}(\lambda_2,\ \bar{\lambda_2})$, is positive. This phenomenon

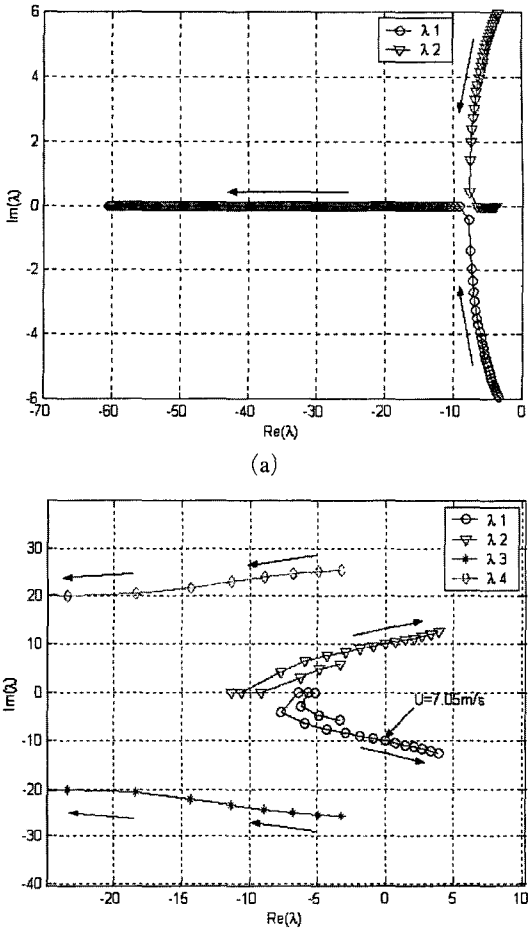

Fig. 2 Argand diagrams for the system ; (a) one-degree-of-freedom model, (b) two-degree-of-freedom model

is called a Hopf bifurcation, and the critical velocity, U is 7.05 m/s. Therefore the lowest dimensional (four-dimensional, two-degree-of-freedom) model is developed in this paper for the simplicity of the continuous system having infinite degrees of freedom.

In order to analyze the system numerically, rendering Eq. (5) into a state-space equation, then the following is obtained.

$$\{\dot{y}\}=[A]\{y\}+\{F(y)\},$$
$$\{y\}=\{q_1,\ \dot{q}_1,\ q_2,\ \dot{q}_2\}^T \quad (8)$$

Eq. (8) is numerically integrated by using fourth

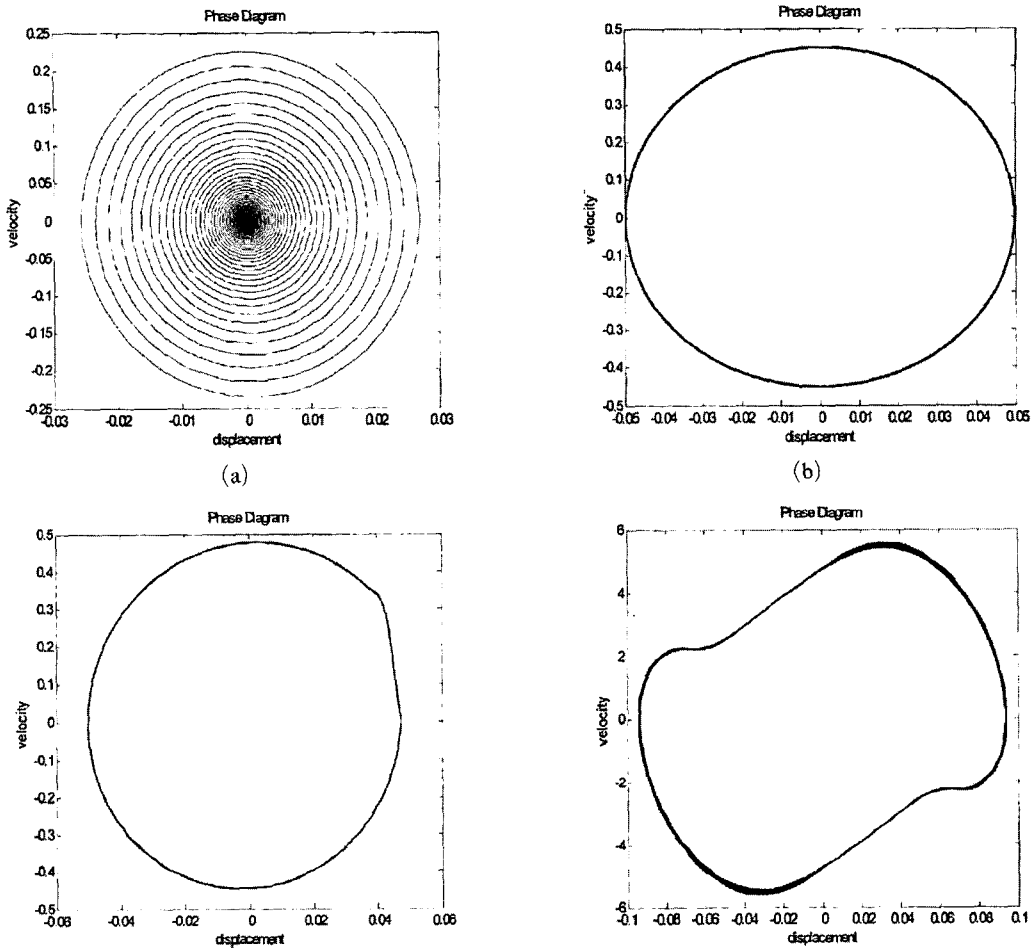

Fig. 3 Phase plane plots of the system ($E=9.72\times10^6$ N/m^2, $E^*=1.723\times10^5$ Ns/m^2); (a) for $U=7.0$ m/s, (b) 7.1m/s, (c) 7.25 m/s, and (d) 30.0 m/s

order Runge-Kutta algorithm with initial conditions, $y_1(0)=y_3(0)=0.01$, $y_2(0)=y_4(0)=0$ and the step size is 0.005. The resultant phase plots with the parameters in Table 1 are shown in Fig. 3. Figure 3 shows that the system is asymptotically stable for $U=7.0$ m/s in (a), the limit cycle motion beyond a Hopf bifurcation for $U=$ 7.1 m/s is observed in (b), and asymmetric limit cycle caused by different initial condition is shown in (c). Figure 3 (d) shows that the system flutters as contacting two sides of the constraints. However, the results show no onset or phenomenon of chaotic motion for the velocities.

The tensile-test is performed to calculate the

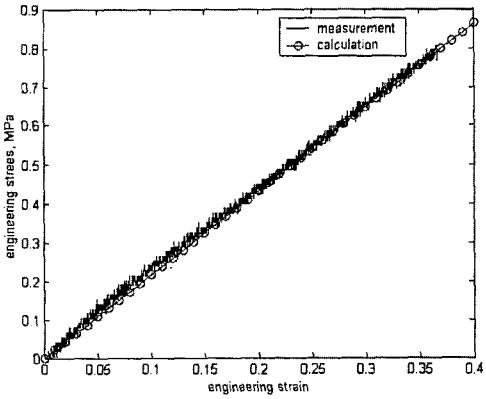

Fig. 4 Engineering stress-strain diagram for the silicon rubber tube

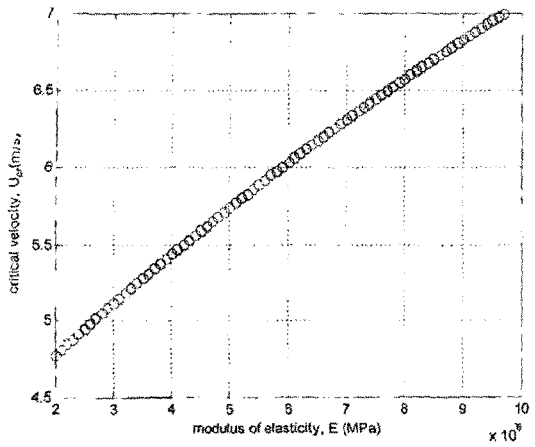

Fig. 5 Critical velocity vs. modulus of elasticity, E

modulus of elasticity of the silicon rubber tube. Figure 4 shows the result of the test, and the calculated value is E=2.159 MPa. Figure 5 shows that the critical flow velocity is proportional to the modulus of elasticity. The critical velocity appropriate to the modulus of elasticity of tested tube is 4.79 m/s. This means that the behavior of the tube can vary with some material properties. The next chapter, examined which critical flow velocity is appropriated to the system with experiments.

3. Experiment of Tube Conveying Fluid

To carry out an experiment for the system, an apparatus is made as shown in Fig. 6 with the parameters of the tube and the fluid in Table 1. The motor of a pump is controlled to vary the flow velocity. As the velocity is increased, the motion of a tube is measured with two laser sensors and analyzed by an FFT analyzer and a PC which can also store the measured data.

The tube being examined in this study becomes unstable by flutter over the critical velocity where a Hopf bifurcation occurs. This state is represented as a limit cycle in a phase plane as shown in Fig. 7.

The amplitude of a limit cycle is proportional to the flow velocity. Therefore, when the motion of the tube is restrained at an appropriate posi-

Table 1 Parameters of the test tube and the fluid

test tube	silicon rubber
fluid	water
length of the tube, L (m)	0.6
outside diameter, d_o (m)	0.011
inside diameter, d_i (m)	0.0076
area moment of inertia, I (m^4)	5.55×10^{-10}
mass of the tube per unit length, m (kg/m)	0.006247
mass of the fluidper unit length, M (kg/m)	0.04527
Young's modulus, E (N/m^2)	9.72×10^6
mass ratio, β	0.87874
coefficient of Kelvin-Voigt damping, E^* (Ns/m^2)	1.723×10^5
laser sensor position, x_{L1}, x_{L2} (m)	0.0766, 0.18165
motion constraint position and gap between the tube and constraint, x_b, y_b (m)	0.28905, 0.0155

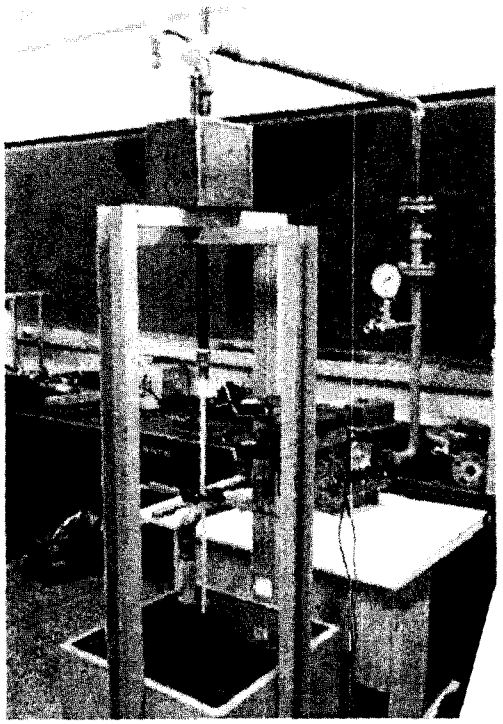

Fig. 6 Photo of the experimental apparat

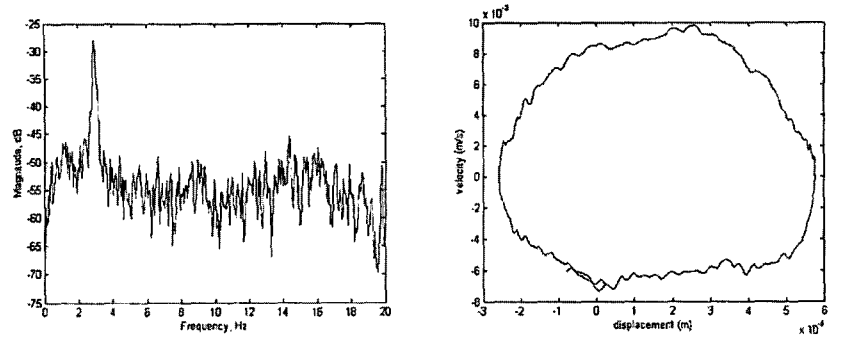

(a)

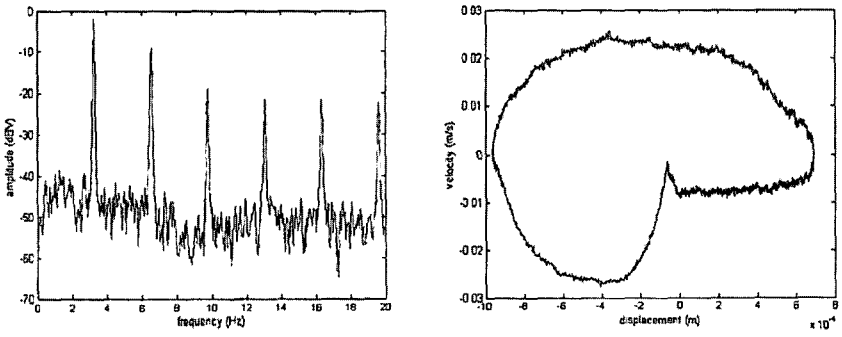

(b)

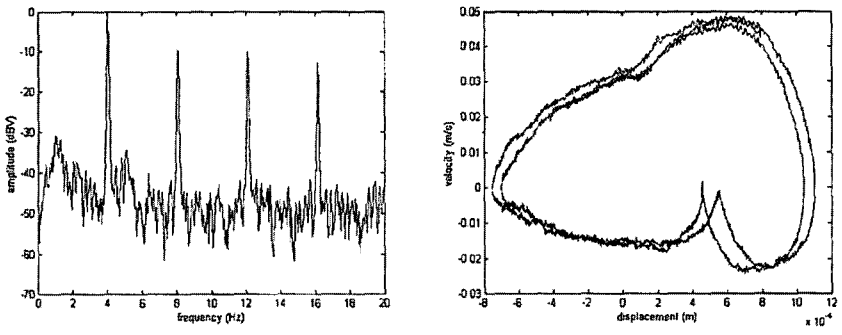

(c)

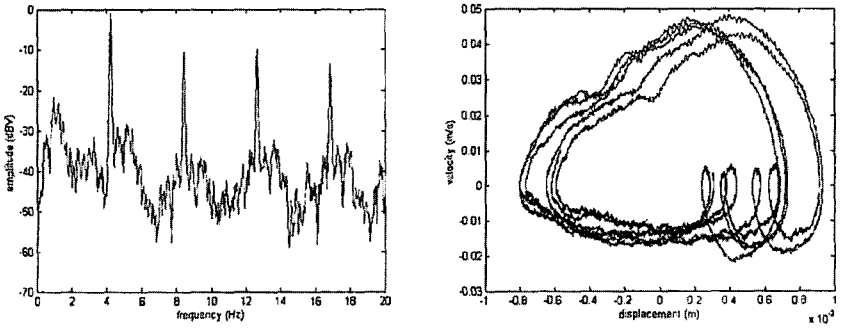

(d)

Fig. 7 Power spectra and phase plots of the system ;
(a) at $U=5.5293$ m/s, (b) 5.6506 m/s, (c) 6.019 m/s, and (d) 6.0927 m/s

tion, the tube bumps against one side of the constraint, but does not contact permanently. A pitchfork bifurcation occurs that a symmetric limit cycle is transformed into an asymmetric one in accordance with the change of the initial condition. Increasing with the flow velocity, a period-doubling bifurcation is generated, which the behavior is multi-periodic. In Fig. 7(a) the tube flutters for the velocity $U>5.52$ m/s without banging on the constraint. The more the velocity increases, the larger the amplitude of the motion becomes, and consequently, higher harmonics components are generated by contacting with the constraint as in (b), and the limit cycle can be shown in the phase plot. It is clearly seen that the subharmonic components of a fundamental frequency occur in (c) and (d), so two or more periodic motions are presented in phase diagrams.

A bifurcation diagram is presented with the displacement of the tube when the velocity of the tube is zero at each flow velocity in Fig. 8. Figure 8 shows that the Hopf bifurcation occurs at $U=$ 5.52 m/s and the period-doubling bifurcation at $U=5.993$ m/s and 6.053 m/s.

The problem which has to be considered is that the critical velocity (Hopf bifurcation occurs) of the experiments is different from one of the numerical analysis with the modulus elasticity, $E=9.72$ MPa as well as one of the numerical analysis with the modulus elasticity calculated from the tensile test (the modulus of elasticity is 2.159 MPa) in the previous chapter. These differences mean that the critical flow velocity when the Hopf bifurcation occurs varies as some material properties. Therefore, exact material properties in the experimental system need to be verified. The exact material properties will be estimated by system identification in the following chapter.

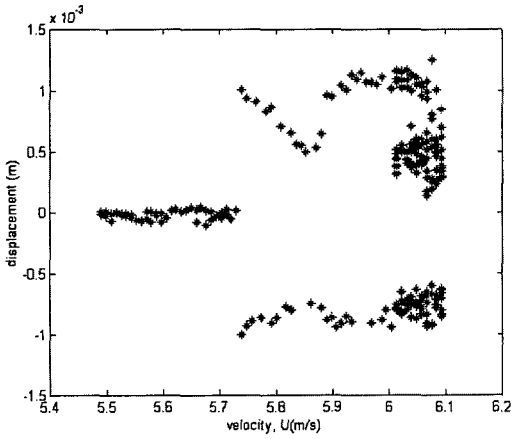

Fig. 8 Bifurcation diagram by the experiment

4. System Identification

The nonlinear dynamic behavior of the tube was observed previously. However, to compare the theoretical analyses of the tube with the experiment results, one exactly defines the parameters that include sensitively variable ones, such as Young's modulus and the coefficient of viscoelastic damping. Accordingly, in this paper, Young's modulus, the coefficient of Kelvin-Voigt damping, and the stiffness of the constraint are estimated with system identification from the data obtained by the experiment.

To estimate the parameters of the system, Eq. (5) is transformed into as follows.

$$\psi=A\cdot\theta \tag{9}$$

That is,

$$\begin{bmatrix} \ddot{q}_1(t_1) & \ddot{q}_2(t_1) \\ \vdots & \vdots \\ \ddot{q}_1(t_n) & \ddot{q}_2(t_n) \end{bmatrix} = \begin{bmatrix} q_1(t_1) & q_2(t_1) & \dot{q}_1(t_1) & \dot{q}_2(t_1) & f(q(t_1)) \\ \vdots & & \ddots & & \vdots \\ q_1(t_n) & q_2(t_n) & \dot{q}_1(t_n) & \dot{q}_2(t_n) & f(q(t_n)) \end{bmatrix} \begin{bmatrix} a_1 a_2 \\ b_1 b_2 \\ c_1 c_2 \\ d_1 d_2 \\ e_1 e_2 \end{bmatrix} \tag{10}$$

where

$$a_r=K_{r1},\ b_r=K_{r2},\ c_r=C_{r1},\ d_r=C_{r2},\ e_r=\kappa\times\phi_r(\xi_b) \tag{11}$$

The data measured with two laser sensors are substituted into Eq. (10), and then the parameters with the identification being utilized by the least square method (Johansson (1993)), i.e., $(A^TA)^{-1}A^T\phi$, are represented in Table 2. The number of data utilized is n=7000.

What needs to be noticed is that the value of coefficient of elasticity and viscoelasticity in Table 2 are different from those in Table 1. This means that the parameters can be varied along the temperature, humidity, and time of being used when the system is operated. In consequence,

there are limits to design the system with only the value of a handbook. Therefore, it needs to validate that parameters used in designing agree with ones in the practical system.

Table 2 Parameters through system identification

Young's modulus, E (N/m^2)	4.041×10^6
coefficient of Kelvin-Voigt damping, E^* (Ns/m^2)	0.8173×10^5
stiffness of the constraint, κ (N/m^2)	783.29

5. Comparison and Verification

The results with the parameters estimated are shown in Figure 9. Here, the tip displacement and velocity of tube are calculated with Eq. (12), and the transients are truncated.

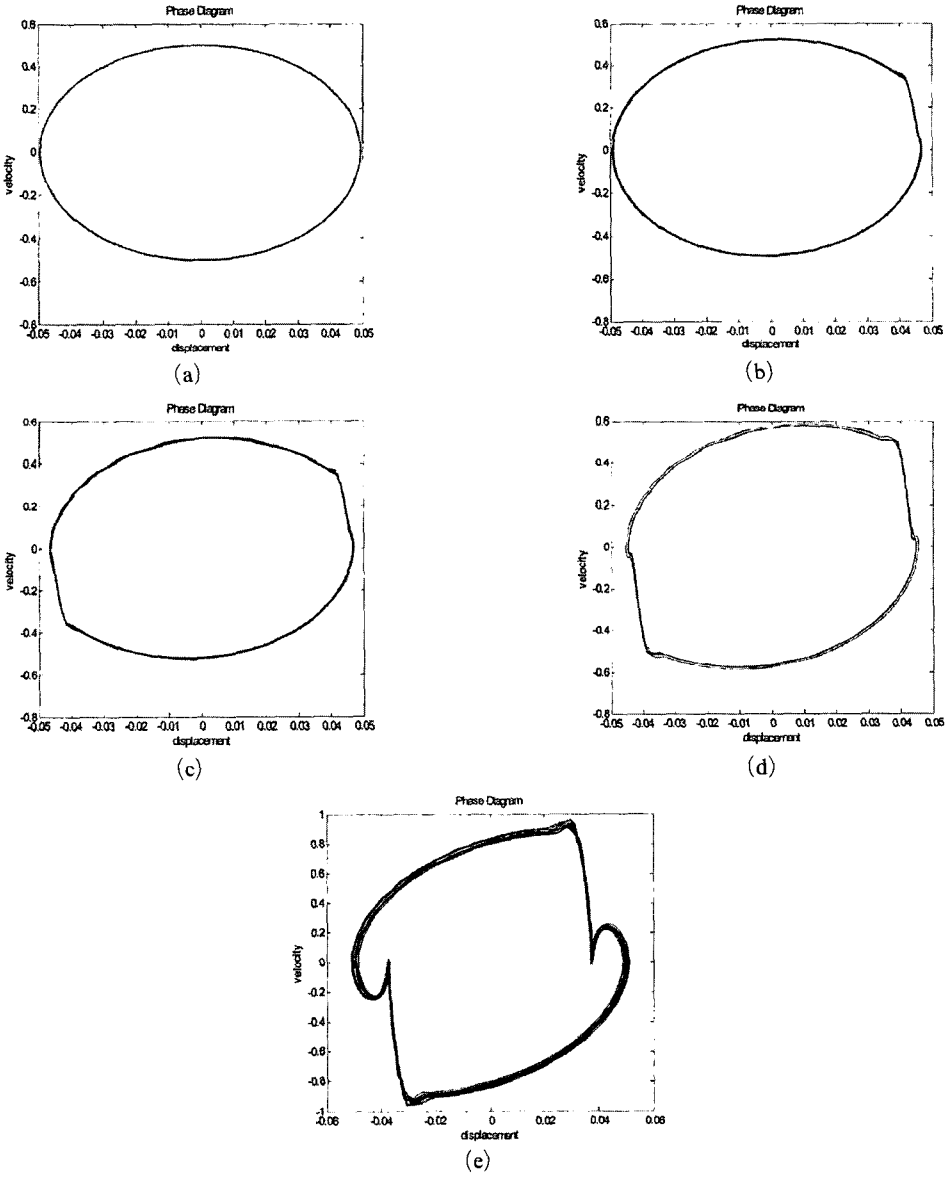

Fig. 9 Phase plots and Poincare map of the system ($E=4.041\times10^6$ N/m^2, $E^*=0.8173\times10^5$ Ns/m^2); (a) at $U=5.457$ m/s, (b) 5.55 m/s, (c) 5.67 m/s, (d) 5.95 m/s, and (e) 6.70 m/s

Table 3 Comparison of experimental and numerical values of the critical flow velocities

U	experiment, A	numerical results, B	$\lvert A-B\rvert/A\times 100$
U_H	5.52 m/s	5.45 m/s	1.27%
U_{pf}	5.65 m/s	5.497 m/s	2.7%
U_{pd}	5.993 m/s	5.948 m/s	0.75%
U_{ch}	-	6.5 m/s	-

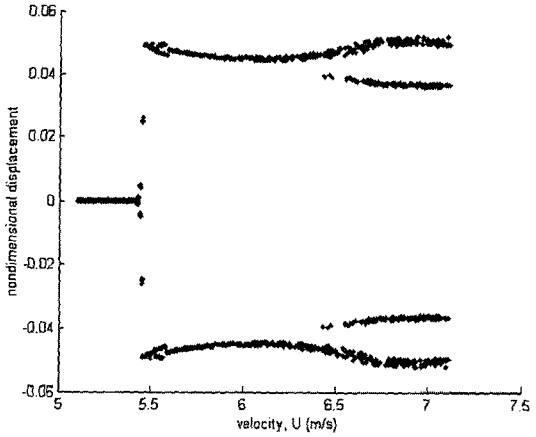

Fig. 10 Bifurcation diagram for the tip displacement of the system for the range of $5.1 \leq U \leq 7.11$m/s

$$\eta(1,\tau) \approx \phi_1(1)\, y_1(\tau) + \phi_2(1)\, y_3(\tau)$$
$$\dot{\eta}(1,\tau) \approx \phi_1(1)\, y_2(\tau) + \phi_2(1)\, y_4(\tau) \qquad (12)$$

In Figures 2, 5, 8, the critical velocity at which the Hopf bifurcation occurs in theoretical and experimental analyses were considerably different from each other, and in Fig. 8 the period doubling bifurcations were verified, while there were not any unstable limit cycles with the parameters in Table 1. But Fig. 9 shows the symmetric limit cycle (a), asymmetric limit cycle (b), a motion contacting the constraint (c), period-double motion (d), and narrow band chaotic motion. The bifurcation diagram with the estimated parameters for the range of $5.1 \leq U \leq 7.11$ m/s when the tip velocity of the tube is zero is represented in Fig. 10. As shown in Fig. 10, there are a little differences between each flow velocity which causes the bifurcations in the experiment and those in numerical results with the estimated

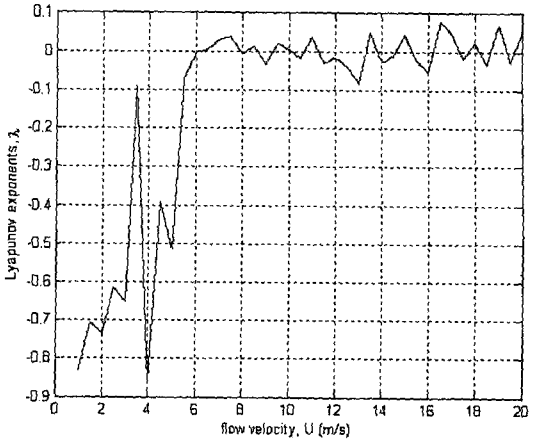

Fig. 11 Lyapunov exponents for the system for the range of $1 \leq U \leq 20.0$ m/s

parameters as in Table 3 (where Hopf bifurcation occurs for U_H, pitchfork bifurcation for U_{pf}, period-doubling bifurcation for U_{pd}, and chaotic motion occurs for U_{ch}) however the overall behaviors of the tube is nearly similar to each other. There are very small differences between the parameters in designing and the parameters being identified, nevertheless remarkable contrasts are appeared in the results. The difference of Young's modulus compared with the value in designing is about 58.4% as 5.679×10^6 N/m^2, and the difference of the coefficient of the Kelvin-Voigt damping is about 52.57% as 0.9057×10^5 Ns/m^2, but the characteristics of the system from each parameter are completely different. This means that the dynamic characteristic of the cantilever tube can be varied along not only the flow velocity being conveyed internally, but also the stiffness and the damping parameter of the tube.

In Fig. 11, the largest Lyapunov exponents were calculated to define the chaotic behavior of the system. As shown in Fig. 11, the motion of the tube becomes chaotic for $U > 6.5$ m/s because the largest Lyapunov exponent, λ is positive. Also, Lyapunov exponents of the range of the coefficient of viscoelasticity, $0.5\times10^5 \leq E^* \leq 5.0\times10^5$ Ns/m^2 for U=8.0 m/s are computed in Fig. 12. Figure 12 shows that the behavior of the tube is varied with the coefficient of viscoelastiity, i.e., chaotic motion of the system occurs for $E^* >$ 1 Ns/m^2.

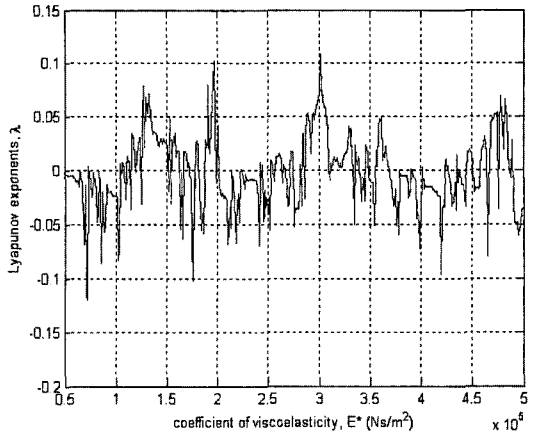

Fig. 12 Lyapunov exponents for $U=8.0$ m/s and the range of $0.5\times10^5\leq E^*\leq5.0\times10^5$ Ns/m^2

Therefore, since a small difference of the stiffness or the damping parameter can affect the entire behavior of the system, such an alteration should not be overlooked.

6. Conclusions

In this study, the nonlinear dynamic behavior of a flexible cantilever tube conveying fluid was examined. As for this, a two-degree-of-freedom model was adopted and an experimental apparatus was made. A system identification was performed to estimate the parameters of the tube, and the parameters were substituted into the equation of motion to compare the results from the numerical analyses and the experimental results.

Since the modulus of elasticity and the coefficient of viscoelasticity can be varied with the environments on which the system operates, there are the differences between the expected behavior while designing and the experimental one.

The characteristic of the cantilever tube system is very sensitive to the parameters. The system with an arbitrary parameter can be destablized by flutterlike divergence, while the chaotic motions can occur in the system with a small change of the material property.

Therefore, when one designs a piping system, it is necessary to consider these two parameters of the modulus of elasticity and the coefficient of viscoelasticity carefully.

References

Ashley, H. and Haviland, G., 1950, "Bending vibrations of a pipeline containing flowing fluid," *Applied Mechanics*, Vol. 17, pp. 229~232.

Benjamin, T. B., 1961, "Dynamics of a system of articulated pipes conveying fluids-1. Theory," *Proceedings of the Royal Society*, Vol. 261 (series A), 457.

Paidoussis, M. P., 1970, "Dynamics of tubular cantilevers conveying fluid," *Journal of Mechanical Engineering Science*, Vol. 12, pp. 65~103.

Sugiyama, Y., Tanaka, Y., Kishi, T. and Kawagoe, H., 1985, "Effect of a spring support on the stability of pipes conveying fluid," *Journal of Sound and Vibration*, Vol. 100, pp. 257~270.

Paidoussis, M. P. and Moon, F. C., 1988, "Nonlinear and chaotic fluidelastic vibrations of a flexible pipe conveying fluid," *Journal of Fluids and Structures*, pp. 567~591.

Paidoussis, M. P., Li G. X. and Moon, F. C., 1989, "Chaotic oscillations of the autonomous system of a constrained pipe conveying fluid," *Journal of Sound and Vibration*, Vol. 135, pp. 1~19.

Chio, Y. S. and Noah, S. T., 1988, "Forced Periodic Vibration of Unsymmetric Piecewise-Linear System," *Journal of Sound and Vibration*, Vol. 121, No. 1, pp. 117~126.

Jin, J. D., 1997, "Stability and chaotic motions of a restrained piped conveying fluid," *Journal of Sound and Vibration*, Vol. 208, pp. 427~439.

Paidoussis, M. P., Li, G. X. and Rand, R. H., 1991, "Chaotic motions of a constrained pipe conveying fluid : comparison between simulation, analysis, and experiment," *Journal of Applied Mechanics*, Vol. 58, pp. 559~565.

Moon, F. C., 1987, Chaotic vibration, John Wiley & Sons, New York.

Johansson, R., 1993, System modeling and identification, Prentice-Hall, New Jersey.